Gofman et al., *Cogent Chemistry* (2015), 1: 1076712
http://dx.doi.org/10.1080/23312009.2015.1076712

cogent chemistry

MATERIALS CHEMISTRY | RESEARCH ARTICLE

Peculiarities of the initial stages of carbonization processes in polyimide-based nanocomposite films containing carbon nanoparticles

I.V. Gofman[1]*, K. Balik[2], M. Cerny[2], M. Zaloudkova[2], M.Ja. Goikhman[1] and V.E. Yudin[1]

Received: 21 January 2015
Accepted: 19 June 2015
Published: 24 August 2015

*Corresponding author: I.V. Gofman, Institute of Macromolecular Compounds, Russian Academy of Sciences, Bolshoy pr. 31, St. Petersburg 199004, Russia
E-mail: gofman@imc.macro.ru

Reviewing editor:
Eugen Stulz, University of Southampton, UK

Additional information is available at the end of the article

Abstract: Carbonization of the polyimide-based composite films containing carbon nanoparticles, namely nanofibers and nanocones/disks, in the temperature range 500–550°C was studied and the kinetics of the initial stage of carbonization and the effect of the filler on the mechanical properties of the carbonized films were evaluated. Two polyimides (PIs) characterized by different macrochains' rigidity and different degrees of ordering of the intermolecular structure were used. The character of the nanofiller's action on the kinetics of the carbonization process depends on the heating rate. In this work, the intensity of the destruction of the PI matrix of the composite films was shown to be slightly higher than that of films of the same polymers with no filler. The introduction of the carbon nanoparticles into both PIs provokes the increase in the ultimate deformation values of the partially carbonized films, while the carbonization of the unfilled PI films yields the brittle materials. The Young's modulus values of the materials based on the rigid-rod PI do not increase after carbonization, while those for compositions based on the PI with semi-rigid chains increase substantially. Carbon nanocones/disks are characterized by the best compatibility with matrix PIs in comparison with carbon nanofibers.

Subjects: Composites; Experimental Physics; Materials Chemistry; Polymers & Plastics

ABOUT THE AUTHORS

The main field of the scientific activity of the research group is concentrated at the investigation of the optimal ways of the polymer-inorganic nanocomposites' formation, the study of the mechanical and thermal properties of the nanocomposite materials obtained, and the clarification of the correlations between these properties and the structure of the nanocomposites under study.

PUBLIC INTEREST STATEMENT

One of the most promising groups of new structural materials for aerospace applications, aviation, automotive industry, shipbuilding, and many other branches of modern techniques are the carbon materials and carbon–carbon composites. These graphite-like materials that are characterized by a high degree of ordering of structure can be obtained by the processes of carbonization–graphitization of polymer precursors. Thus, the key question of the subject is the selection of the polymer materials that are the optimal starting systems to insure the carbon materials with the best quality. The investigations carried out up to date have shown that polymers that belong to the group of aromatic polyimides are the excellent precursors for the production of high-quality carbon materials. In the work presented, the possible ways are investigated to optimize the carbonization process by introducing the carbon nanofillers into the polyimide precursors.

Keywords: carbonization; polyimides; nanocomposite films; carbon nanocones/disks; vapor grown carbon fibers

1. Introduction

One of the promising directions of the progress in contemporary materials science, which makes it possible to obtain thermally stable and durable materials with low density, is the development of carbon materials. These materials are now widely used in different branches of modern techniques including aerospace engineering, aviation, shipbuilding, automotive industry, instrumentation, and others.

High-quality carbon materials can be produced by the appropriate thermal treatment of different polymeric precursors or polymer–carbon compositions. The large number of studies carried out in recent years to investigate the carbonization–graphitization processes showed that the properties of carbon materials obtained this way significantly depend on the type of the polymeric precursor, namely on its chemical structure and supramolecular organization. So, the important problem of modern polymer science is to select the types of polymer matrices that, under the appropriate thermal treatment, can be converted into the graphite-like carbon materials with the optimal structure and properties.

One of the most promising classes of the polymers, utilized as the precursors, is that of the aromatic polyimides (PIs) (Bessonov, Koton, Kudryavtsev, & Laius, 1987). Basing on PIs, it is possible to obtain graphite-like carbon materials with high degree of order of the supermolecular structure and extremely high coke residue (Doyama et al., 2003; Luo & Matsuo, 2010; Smirnova et al., 2007; Takeichi, Endo, Kaburagi, Hishiyama, & Inagaki, 1998).

The processes of the initial polymers transformation into the carbon materials take place in the wide temperature range of 2,700–2,800°C, but the important role in the formation of the final material with optimal characteristics belongs to the initial stage of the heat treatment of the PI precursor in the range of 500–700°C. It was shown (Dobrovol'skaya, Mokeev, Sazanov, Gribanov, & Sukhanova, 2006; Doyama et al., 2011; Gribanov, Sazanov, & Mokeev, 2002) that deep structural and chemical transformations of the starting PIs occur in this temperature range to form the "green product" of future graphite-like materials.

The additional possibilities to optimize the properties of the products of carbonization–graphitization of PI materials are provided by the introduction of some types of carbon particles into the polymeric precursors. It was shown that these nanoparticles, being exfoliated in the polymer volume, can provoke the deep variations of the supramolecular structure of the polymer matrices (Peponi, Puglia, Torre, Valentini, & Kenny, 2014; Zhang et al., 2012). But to date, the character of the influence of these nanoparticles on the polymer carbonization processes is not yet clear . The impact of carbon nanoparticles of different types on the thermally stimulated processes, which pass in the PI-based composite films at the early stages of carbonization, and on the properties of these films in the carbonized state are investigated in this work.

2. Experimental

2.1. Preparation of PI films and PI-based composite ones

Films of two PIs based on 3,3′,4,4′-biphenyltetracarboxylic dianhydride and *p*-phenylenediamine or on piromellitic dianhydride and 4,4′-oxydianiline (denoted below as PI-I and PI-II, respectively) were used as matrix polymers. Following are the molecular structures of these PIs:

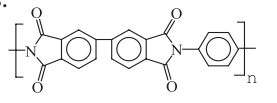

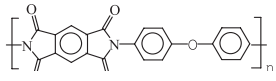

As the nanofillers for these matrix PIs, two types of carbon particles were used: vapor-grown carbon fibers (VGCF) (http://www.sdkc.com/documents/VGCF-H.pdf) or carbon nanocones/disks (CNC) (http://www.n-tec.no/en/Topmenu/Products/Carbon-cones.aspx). Before being introduced into the polymer solutions, the nanoparticles were pre-dried during 30 min at 150°C in the inert atmosphere.

The two-steps synthesis method (Bessonov et al., 1987) was used to obtain both the starting PI films and PI-based composite ones. The synthesis of pre-polymers—poly(amic acids) (PAAs) was described in details elsewhere (Bessonov et al., 1987). The PAA films were produced by casting the solutions of PAAs in 1-methyl-2-pyrrolidinone (N-MP) onto glass plates with the subsequent thermal treatment at 80°C for 3 h. The resulting samples thickness was 30–40 μm and the residual solvent content in the films was as high as 20 wt. %. Curing was achieved by heating these PAA films on the glass plates at the rate of 5 deg/min up to 360°C (for PI-II) or up to 400°C (for PI-I) with subsequent thermal treatment at these temperatures for 20 min. The treatment above leads not only to the PAA conversion into PI, but, on another hand, to the complete removal of any residual amounts of low molecular weight products (such as solvent, water) from the film.

To obtain the composite materials, the dispersions of VGCF or CNC in N-MP, produced by the ultrasound method, were added to the PAA solutions with the subsequent homogenization of the mixture by the mechanical overhead stirrer. The PI-based composite films were produced from these composite solutions as described above.

2.2. Graphitization of PI and composite films

All samples of the PI and PI-based composite films under study were subjected to the thermal treatment to provoke the initial stages of carbonization. These films were heated up to 500 or 550°C at the rate of 0.8–1.0 deg/min in the flow of nitrogen and then kept at the appropriate temperature for 1 h in the same atmosphere.

2.3. Measurements of the films' properties in pristine and partially carbonized states

Mechanical characteristics of the green polymer and composite films were determined under the conditions of uniaxial extension using band-like samples of 2-mm width and 25-mm long. Experiments were carried out on AG-100kNX universal mechanical tests system (Shimadzu, Japan). Mechanical characteristics of the carbonized films were determined under the same deformation mode using band-like samples of 5-mm width and 40–50-mm long. Experiments were carried out on the universal testing machine, Inspekt 100 (Hegewald-Peschke, Germany).

In both cases, the extension speed was 10 mm/min.

The Young's moduli E, tensile strengths σ_b, and ultimate strains ε_b of the materials under study were determined by the mechanical tests.

The densities of the PI-I and PI-II films (ρ) were determined by the flotation method using the laboratory-made measurement unit. The mixtures of toluene and CCl_4 were employed to equilibrate the specimen at 20°C. Both these experimental values of the film density ρ_{exp} and calculated values of van der Waals density of the polymers were used to calculate the values of molecular packing coefficient k (Askadskii, 2003, 2005; Bessonov et al., 1987), characterizing the mean degree of molecular structure ordering of these PI films.

The thermogravimetric measurements (TGA) in the temperature range RT-800°C were conducted using 5–10-mg film samples contained in Al_2O_3 crucibles in nitrogen atmosphere. The TG 209 F1 Iris microbalance (NETZSCH, Germany) was used for these tests. TGA data were used to determine the thermal stability indices of the materials studied, i.e. the temperatures (τ_1, τ_5, and τ_{10}) at which the sample's weight reduces in, respectively, 1, 5, and 10 wt. % under the thermal destruction processes.

The mass spectroscopy of gaseous products of the thermally stimulated destruction of the films under study was carried out using TA-QMS 403 C Aëolos mass spectrometer (NETZSCH, Germany).

The SEM images of both pristine and carbonized films of PIs and PI-based composites were obtained using Qanta 450 scanning electron microscope (FEI, USA) in high vacuum mode with Everhart-Thornley detector.

3. Results and discussion

3.1. The kinetics of the carbonization process of the PI and composite films

The first question to be clarified during this work concerned the influence of the nanoparticles, introduced into the PI matrix, upon the kinetics of the carbonization process. This information can be obtained by the comparative TGA measurements of the PI films and PI-based compositions with different concentrations of nanoparticles. Indeed, the process of mass depression during the sample's heating in the temperature range under consideration, registered by TGA, caused by the stepwise release of the volatile products of the destruction, reflects both the variations of the chemical structure of the material under study and the rearrangements of the material's supramolecular structure that take place during this destruction process (Doyama et al., 2011; Gribanov et al., 2002; Smirnova et al., 2007).

At the first stage of our work, we have carried out these tests in the standard TGA regime (heating in the inert medium with the rate of 5 deg/min) to clarify the main features of the process. The results of these comparative tests for the PI-II film and PI-II-CNC composite one are presented in Figure 1.

The obtained results testify the complex nature of the influence of dispersed carbon nanofiller on the process of the thermal destruction of the polymer. The introduction of CNC into the PI film definitely leads to the acceleration of the thermal destruction process of the material at the early stages, namely at the temperature range up to 600–650°C (Section I of the TGA curves, Figure 1). The inverse effect is observed in the region of temperatures above 650°C (Section II of the TGA curves, Figure 1): the rate of mass changes of the samples decreases along with the increase in the concentration of CNC. The same effects were registered while studying the thermal destruction of the PI-VGCF composite films.

Thus, it could be assumed, basing on the results of these tests, carried out in the "standard" TGA conditions, that in the temperature range in which the carbonization of the investigated samples was conducted (500–550°C), the presence of nanoparticles of both types in the PI accelerates the destruction processes. The comparison of the indices of thermal stability (Table 1) indicates this fact clearly. Consequently, it could be assumed that the process of the carbonization of the composite films studied led to more substantial changes in the structure of precursor than the process of the carbonization of the unfilled PI films carried out under the same conditions (the same heating rate and final temperature) (Doyama et al., 2011; Gribanov et al., 2002; Smirnova et al., 2007).

However, as our further studies showed, the depth of reorganizations of the precursor's structure in the carbonization process depends strongly upon the speed of the film heating during the heat treatment. Figure 2 shows the curves of the mass changes of the PI-II film in the process of further TGA experiment, which imitates the regime of carbonization (heating up to 500°C and subsequent treatment for 1 h at this temperature) with different heating rates. With the reduction of the heating rate from 5 to 0.8 deg/min, the mass losses of the samples in the course of heating increase from ~2 to ~15%. The subsequent isothermal process during 1 h provokes the additional loss of the samples mass as high as ~6.5–7%. Thus, under the conditions of the precursor's heat treatment used in our work (low heating rate), the processes of carbonization and structural rearrangements proceed mainly in the course of the samples' heating up to the final temperature.

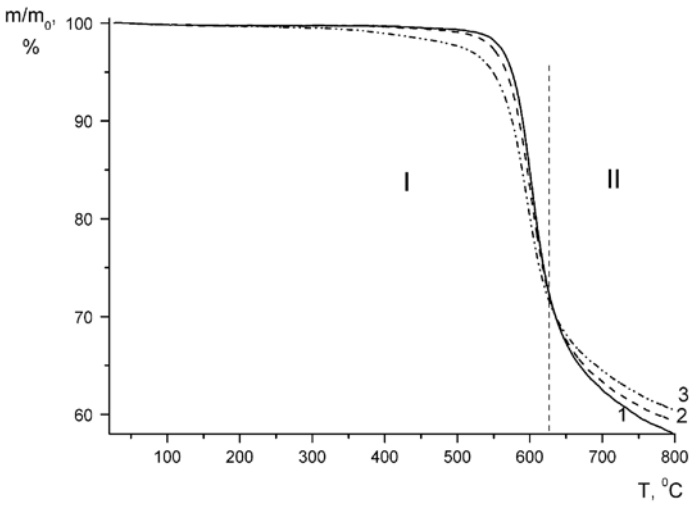

Figure 1. TGA curves (heating in the inert medium with the rate of 5 deg/min) of the PI-II film (1) and the composite films PI-II + 3% CNC (2), and PI-II + 6% CNC (3).

Table 1. Indices of thermal stability of the films of PI-II and composites of PI-II with CNC ("standard" test conditions—heating speed 5 deg/min)

N	PI and nanoparticles types, nanoparticles concentration (vol. %)	τ_1 (°C)	τ_5 (°C)	τ_{10} (°C)
II	PI-II	541	576	590
II-I	PI-II + 3 % CNC	524	570	585
II-II	PI-II + 6 % CNC	456	555	577

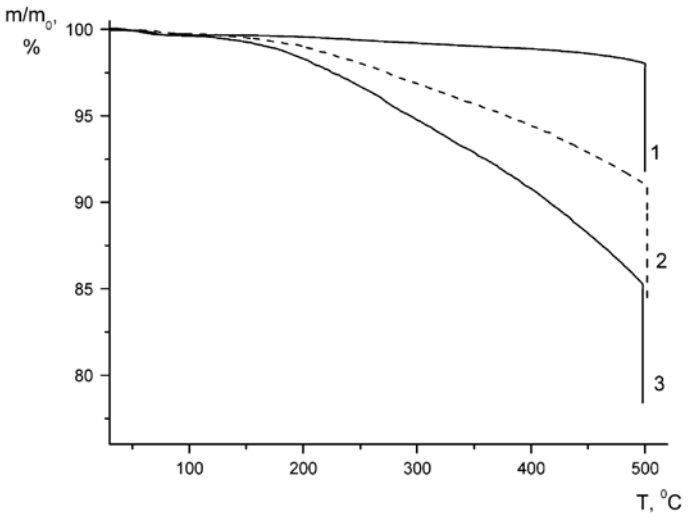

Figure 2. TGA curves of the PI-II film at different temperature–time regimes: heating up to 500°C with rates of 5 deg/min (1), 2 deg/min (2), and 0.8 deg/min (3) with subsequent treatment for 1 h at 500°C.

Further comparison of the TGA curves of the PI-II films and of the compositions on the basis of this PI, containing 6% CNC, obtained in the regime of samples heating, which imitates the process of carbonization (low heating speed, Figure 3), showed that after considerable reduction in the heating rate, it is possible yet to distinguish two well noticeable sections of the TGA curves. Namely, in the low temperature region (Section I of the TGA curves, Figure 3), the processes of the mass loss proceed more intensively in the composite films, and with the increase in temperature, the PI films begin to destruct more rapidly than the composite ones (Section II of the TGA curves, Figure 3). This result seems to be similar to that presented in Figure 1. However, in the case of the low heating speed, the boundary

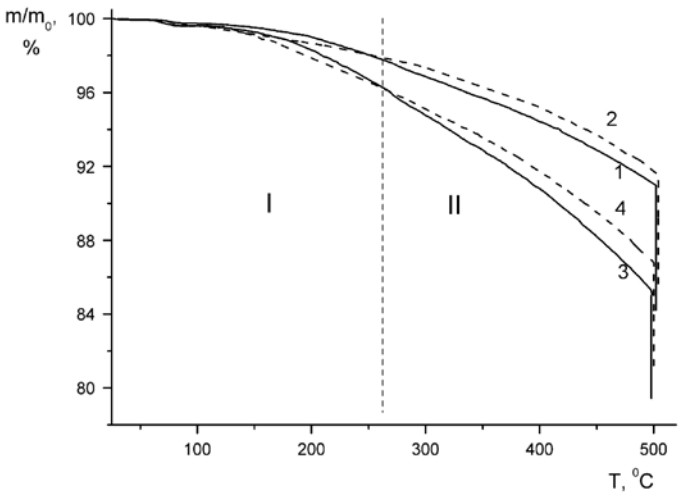

Figure 3. TGA curves of the PI-II films (1, 3) and the PI-II + 6% CNC composite films (2, 4) at different temperature–time regimes: heating up to 500°C with rates 2 deg/min (1, 2) and 0.8 deg/min (3, 4) with subsequent thermal treatment for 1 h at 500°C.

between these two regions is shifted sharply into the low temperature region. In the case of samples heating with the rate as low as 0.8 deg/min (regime, corresponding to the conditions of the carbonization process), the destruction of composite films occurs more slowly than the destruction of unfilled PI-II, already after ~260°C.

As a result, the described experiments showed that during the carbonization of the composite films (PI-II + 6% CNC) in the regime, used in the work, the depth of destruction occurs to 1.5–1.8% less than during the carbonization of the unfilled PI film.

The difference in the mass losses upon the carbonization of the composite films and of the PI ones correlates reasonably with the nanoparticles' concentration in the material: from ~0.5% for the material with the filler concentration 1% up to ~2.6–3% for the composite films containing 9% of nanoparticles.

The results similar to those presented in Figure 3 were obtained during the TGA of the composite films based on PI-I: the destruction of composite film, containing 6% CNC, occurs more slowly than the destruction of unfilled PI-I, at the temperatures above ~270°C.

Basing on the data above, the conclusion can be drawn that the introduction of the carbon nanoparticles in the polymer volume provokes the retardation of the thermally stimulated destruction of the material. But, while treating these results, we should take into account the fact that during the heating of the composite films, only the destruction of the polymer matrix takes place, while the second component of the system, the nanofiller, is stable in the temperature region under study. Hence, to estimate the kinetics of the process studied, it would be correct to use the mass of only polymeric part of the composite material as the base mass value while calculating the percents of the mass losses.

While we have calculated the "real mass losses" by this method, we have seen that the intensity of the thermally stimulated destruction of the matrix PIs during the thermal treatment of the composite films studied is a little higher than that of the unfilled PI films. For example, the amount of coke residue of the polymer in the composition PI-II + 6% CNC at the end of the carbonization process, presented in Figure 3, is about 0.5% less than that of the unfilled PI-II film.

The results of mass spectrometry did not reveal any noticeable differences in the composition of the gaseous products that are released during the destruction of the unfilled PI films and of the PI-based composites. In all cases, during the carbonization process, the volatilization of water, CO_2, and some minor amount of CO was registered in the temperature range above ~450°C. These results are

in good agreement with that reported in Perng (2000) while studying the carbonization of the Ultem poly(ether imide). All these gaseous products typically result from the initial stage of the thermal destruction of the PI materials.

No noticeable differences were detected in our work in the concentrations of the above-mentioned gaseous products while studying the thermal destruction of both PIs and PI-based composite films.

3.2. Characterization of the carbonized films

While evaluating the properties of the materials, obtained by the carbonization process, we should remember that two PIs, selected as the initial polymers precursors and as the matrix polymers for the composites formation, are characterized by the different rigidities of the molecular chains. Namely, PI-I is the rigid-chain polymer, containing no hinged atoms and groups in the elementary units, while PI-II has the semi-rigid chains, containing hinged atoms of oxygen in the elementary units. This difference of chemical structures determines the essential differences in the mechanical characteristics of the corresponding PI films (Table 2), first of all—in their hardness. Actually, the Young's modulus of the rigid-chain PI-I film exceeds thrice the modulus of the PI-II film.

This difference testifies the realization of a more advanced system of intermolecular bonds in the PI-I films in comparison with the PI-II ones, which, in turn, corresponds to the more regular supramolecular organization of the PI-I films. We should take into account this difference of the properties of two matrix polymers used while studying the impacts of the nanofillers upon these properties, both in the initial and in the partially carbonized states.

The conclusion above is confirmed by the results of the calculations of the molecular packing coefficients k (Askadskii, 2003, 2005; Bessonov et al., 1987) of the films compared. Actually, the experimental values of the density of the PI-I and the PI-II films were found to be 1.470 and 1.409 g/cm^3, respectively, that correspond to the values of $k = 0.724$ (PI-I) and $k = 0.689$ (PI-II). This difference in the k values of the compared precursor films is substantial, if one considers that the value of $k = 0.683$ characterizes the polymer with the completely amorphous structure, and $k \approx 0.755$—polymer with the completely crystalline one (Askadskii, 2003, 2005). Keeping in mind the results obtained while studying the influence of the degree of order of PI precursor's structure on the characteristics of its carbonization and graphitization products (Inagaki & Feiyu, 2006; Takeichi, Eguchi, Kaburagi, Hishiyama, & Inagaki, 1999), we can conclude that the PI-I film is more promising as a precursor for obtaining the carbon material. It is well known (Bessonov et al., 1987) that the rigid-chain PI films are characterized by the mesomorphic type of supramolecular structure with sufficiently high average degrees of ordering.

Really, the comparison of the mechanical characteristics of two PI films subjected to carbonization at 500°C during 60 min (Table 3) shows the presence of residual ultimate deformation ε_b at the level of ~0.5% for carbonized PI-I film (in this case, only a modest increase of the Young's modulus of PI-I film is registered as a result of carbonization: from 9.3 up to 10.8 GPa), while carbonization of the PI-II film in the same regime brings the absolutely brittle film. However, it is necessary to note that the conclusions, made by the authors (Takeichi et al., 1999), concern the properties of the final products of carbonization–graphitization of PIs, whereas at the intermediate stages of this process, the correlation of the properties of the material with the structure of PI precursor can be expressed not so unambiguously.

However, as it was shown in Smirnova et al. (2007), to obtain high-quality carbon materials with the regular graphite-like structure from PI precursors, it is very important to insure the increased level of the average structural ordering of the initial PI. But it is not enough to solve the problem. It is not less important to ensure the presence of the highly ordered regions as crystallites in the volume of the polymer, which serve in the carbonization process as the centers, ensuring the realization of the mutually regulated arrangement of the hexagonal carbonic structures through all polymer volume.

Table 2. Mechanical properties of the PI and PI-based composite precursor films

N	PI and nanoparticles type, nanoparticles concentration (vol. %)	Films properties			
		E (GPa)	E/E_0 [a]	σ_b (MPa)	ε_b (%)
I	PI-I	9.29 ± 0.28	1	405 ± 8	30 ± 3
I-I	PI-I + 3 vol. % VGCF	9.30 ± 0.19	1.001	353 ± 7	10 ± 1
I-II	PI-I + 6 vol. % VGCF	9.32 ± 0.16	1.003	262 ± 7	8.8 ± 0.7
I-III	PI-I + 3 vol. % CNC	10.44 ± 0.48	1.12	250 ± 24	4.7 ± 0.4
I-IV	PI-I + 6 vol. % CNC	11.09 ± 0.21	1.19	186 ± 24	2.9 ± 0.3
II	PI-II	2.94 ± 0.06	1	156 ± 4	68 ± 2
II-I	PI-II + 3 vol. % VGCF	3.23 ± 0.11	1.1	142 ± 4	32 ± 2
II-II	PI-II + 6 vol. % VGCF	3.62 ± 0.15	1.23	134 ± 5	12 ± 3
II-III	PI-II + 15 vol. % VGCF	4.29 ± 0.11	1.46	111 ± 3	5 ± 1
II-IV	PI-II + 6 vol. % CNC	3.83 ± 0.11	1.30	115 ± 4	8 ± 1

[a] E_0 denotes the Young's modulus of the unfilled polymer film.

Table 3. Mechanical properties of PI-I and PI-II films in initial and partially carbonized states

N	Type of the film	Films properties		
		E (GPa)	σ_b (MPa)	ε_b (%)
I	PI-I	9.29 ± 0.28	405 ± 8	30 ± 3
I-C	PI-I + carbonization up to 500°C	10.82 ± 0.32	28 ± 3	0.5 ± 0.1
II	PI-II	2.94 ± 0.06	156 ± 4	68 ± 2
II-C	PI-II + carbonization up to 500°C	Brittle film		

Introduction of carbon nanoparticles with the ordered structure into the polymer matrix is one of the ways to create such ordered zones in the volume of the PI precursor. To carry out the experimental study of the results of this modification of the polymers precursors, the carbon nanoparticles of two types (VGCF and CNC) were introduced into the PI-I and PI-II matrices.

A study of the mechanical properties of the composite films obtained this way showed that the materials under consideration follow the general tendencies observed while incorporating the nanoparticles with high aspect ratio values into the polymer matrices (the increase in the Young's modulus with simultaneous reduction of the ultimate deformation) (Gofman et al., 2007; Valenkov, Gofman, Nosov, Shapovalov, & Yudin, 2011; Xie, Mai, & Zhou, 2005). However, the concrete manifestations of these tendencies depend on the type of PI matrix (Table 2). Actually, the incorporation of the nanoparticles of both types into the PI-II leads to a noticeable increase in the Young's modulus of the material. Moreover, more considerable increase in *E* (as high as 1.3 times for 6 vol. % of nanoparticles) is registered while CNC were introduced in this PI. On the other hand, the incorporation of the nanoparticles in the PI-I leads to much weaker increase of *E*: use of VGCF in the concentrations up to 6 vol. % as a filler practically does not lead to the increase of *E*, and after the incorporation of CNC in the same

concentration (6 vol. %), the Young's modulus grows only by 19%. Approximately equal reductions of ε_b values are caused by the incorporation of the nanoparticles into both PIs.

One of the basic tasks, which should be performed during the composite processing, is to ensure the maximally uniform distribution of the filler in the volume of the polymeric matrix without the formation of the aggregates of nanoparticles (Valenkov et al., 2011). SEM images of the fracture surfaces of the composite films (Figures 4 and 5) show that the nanoparticles are distributed quite uniformly in the polymeric matrices. No sizable aggregates and bundles of VGCF or CNC can be detected while examining the microphotos obtained.

Table 4 presents the mechanical characteristics of the partially carbonized PI-I- and PI-II-based composite films. The results obtained show that the process of partial carbonization (500°C–60 min) provokes the different changes of the Young's modulus of the composite films based on the two PIs used. The carbonization of the composite films based on the rigid-chain PI-I in all cases (both types of the used carbonic nanoparticle and different concentrations of filler) led to the certain reduction in the Young's modulus of a film as high as 5–10%. The opposite result is observed for the compositions on the basis of the PI-II: the carbonization of the composite films in all cases leads to a considerable increase in the Young's modulus of the material (the *E* grows as high as 40–45% as a result of the carbonization of the composite films containing 6 vol. % of nanoparticles of both types).

The incorporation of the nanoparticles into both PI matrices obviously leads to the increase in the deformability of the films in the partially carbonized state, as compared to that of the partially carbonized unfilled films (Table 4). Actually, the carbonization of the unfilled PI-I films (500°C–60 min) led to

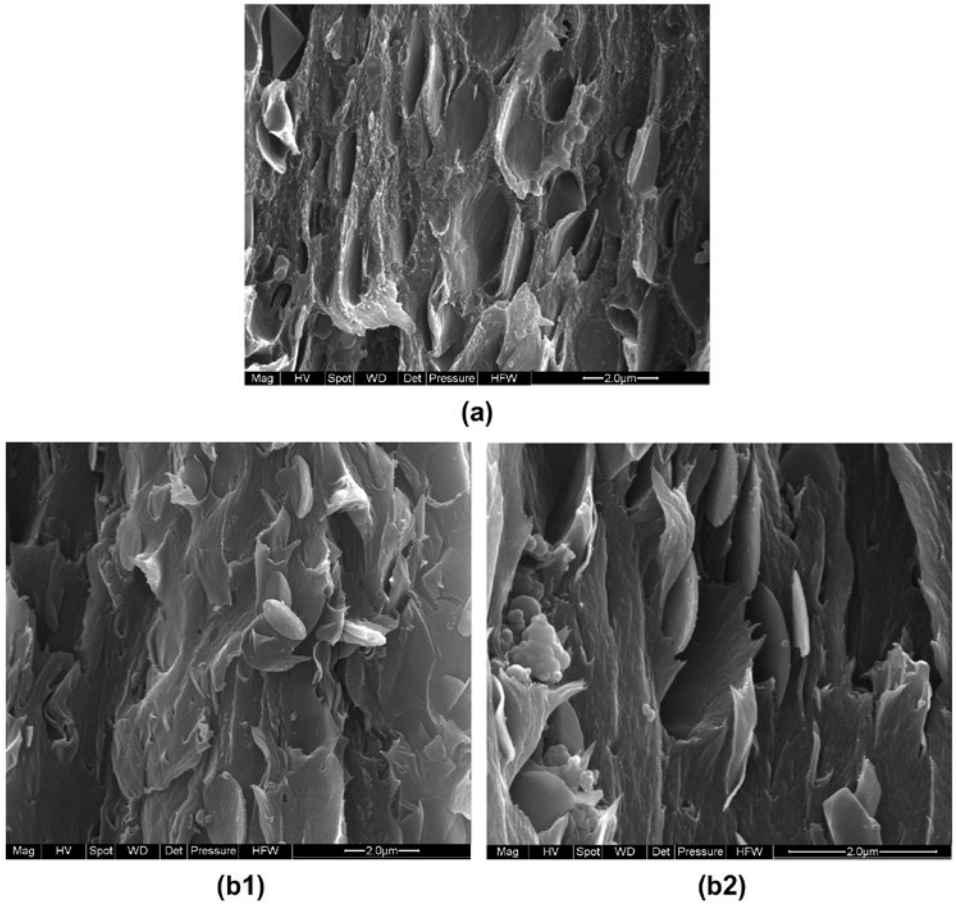

Figure 4. SEM images of failure surfaces of composite films PI-I + 6 vol. % CNC (a) ×5000) and PI-II + 6 vol. % CNC (b) 2 fragments, ×5000 and ×10000).

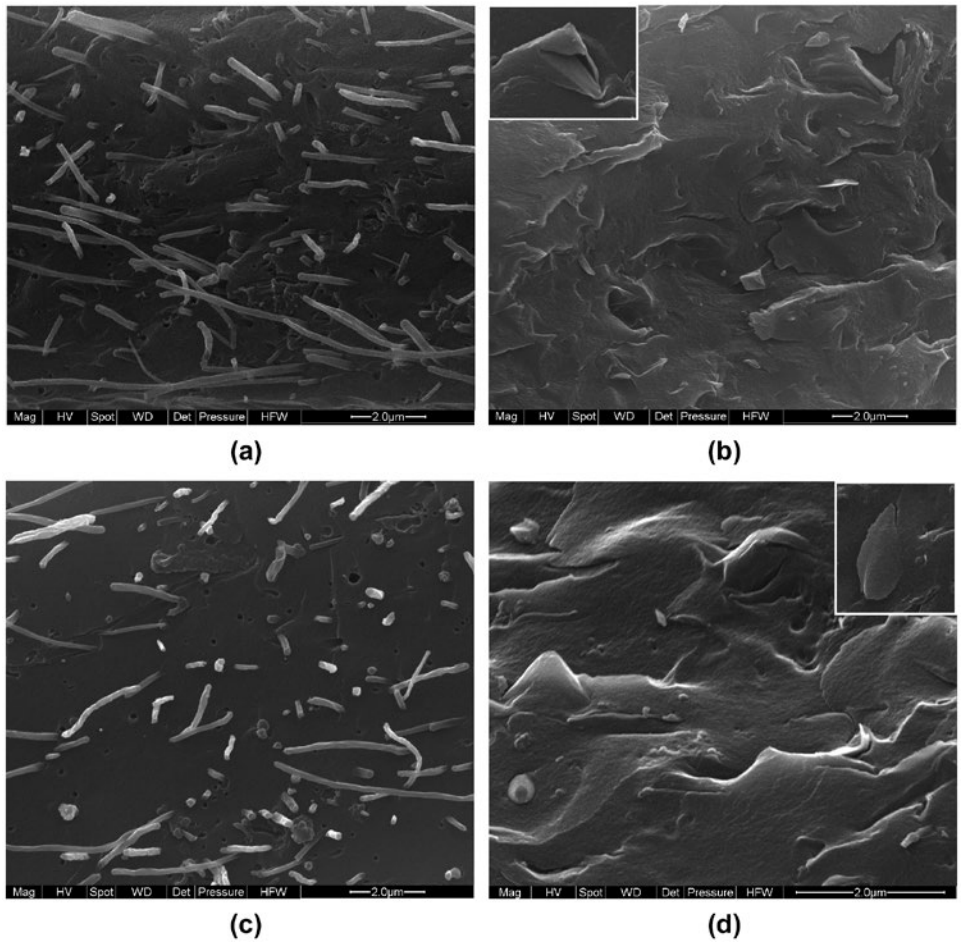

Figure 5. SEM images of failure surfaces of partially carbonized composite films on the base of PI-I (a, b,) and PI-II (c, d), filled by 6 vol. % VGCF (a, c) or 6 vol. % CNC (b, d); a, b, c, – ×5000, d – ×10000; the inserts in (b) and (d) present the destructed CNC on the failure surface.

Table 4. Mechanical properties of the PI-based composite films in both initial and partially carbonized (up to 500°C) states

N	Film type	Films properties		
		E (GPa)	σ_b (MPa)	ε_b (%)
I-II	PI-I + 6 vol. % VGCF	9.32 ± 0.16	262 ± 7	8.8 ± 0.7
I-II-C	I-II + carbonization up to 500°C	8.27 ± 0.18	102 ± 17	1.6 ± 0.5
I-III	PI-I + 3 vol. % CNC	10.44 ± 0.48	250 ± 24	4.7 ± 0.4
I-III-C	I-III + carbonization up to 500°C	10.11 ± 0.21	121 ± 19	1.8 ± 0.4
I-IV	PI-I + 6 vol. % CNC	11.39 ± 0.21	186 ± 24	2.9 ± 0.3
I-IV-C	I-IV + carbonization up to 500°C	10.82 ± 0.32	101 ± 8	0.9 ± 0.2
II-I	PI-II + 3 vol. % VGCF	3.23 ± 0.11	142 ± 4	32 ± 2
II-I-C	II-I + carbonization up to 500°C	3.86 ± 0.24	22 ± 2	0.6 ± 0.1
II-II	II + 6 vol. % VGCF	3.62 ± 0.15	134 ± 5	12 ± 3
II-II-C	II-II + carbonization up to 500°C	5.09 ± 0.12	54 ± 6	1.2 ± 0.2
II-III	PI-II + 15 vol. % VGCF	4.29 ± 0.11	111 ± 3	5 ± 1
II-III-C	II-III + carbonization up to 500°C	5.26 ± 0.06	57 ± 5	1.7± 0.3
II-IV	PI-II + 6 vol. % CNC	3.83 ± 0.11	115 ± 4	8 ± 1
II-IV-C	II-IV + carbonization up to 500°C	5.6 ± 0.2	59 ± 5	1.3 ± 0.2

the formation of materials with ε_b, which does not exceed 0.5%, and during the carbonization of the PI-II, absolutely brittle films were obtained (Table 3). During the carbonization of composite films on the basis of the PI-I under the same conditions, the films with ε_b = 1.8% (composition with 3 vol. % CNC) were obtained.

The same effects are observed during the carbonization of composite films based on the PI-II (Table 4). Moreover, for the films containing VGCF, the tendency of the sequential increase in the deformability of carbonized films along with the increase in the filler concentration in it is outlined clearly: from ε_b = 0.6% for the composition, which contains 3 vol. % of VGCF, to ε_b = 1.7% for the composition with 15 vol. % of VGCF.

Of course the carbonization of the composite films in all cases led to noticeable reduction in their deformability, but it is necessary to note the tendency which can be clearly seen for the compositions on the basis of the PI-II: in proportion to the increase in the concentration of nanoparticles, the relative reduction in the ε_b value during the carbonization of film decreases essentially (Table 4). Really, the carbonization of the PI-II film with 3 vol. % VGCF results in 50 times decrease of ε_b, for the composition of PI-II with 6 vol. % VGCF—only 10 times, and for the composition which contains 15 vol. % VGCF ε_b falls less than three times.

Table 5 presents the mechanical characteristics of the composite films on the basis of PI-II, depending on the maximal temperature T_{max} of the precursor heating during the carbonization process. It is evident that the increase in T_{max} by 50° up to 550°C leads to the considerable increase in the Young's modulus of partially carbonized film; moreover, this increase of E is more noticeable for composites with high concentration of nanoparticles (namely of VGCF). At the same time, the increase in T_{max} leads to further reduction in the deformability of the film. Indeed, after heat treatment at 550°C during 60 min, the ε_b value of the composite films becomes less than 1% even in the case of the maximum concentration of nanoparticle in the matrix (15 vol. % of VGCF).

Microphotos of the fracture surfaces of partially carbonized films on the basis of both PI matrices (Figure 5) demonstrate clearly the best compatibility of CNC with the matrix PIs in comparison with VGCF. Actually, the long fragments of the fibers, pulled out from the matrix, and the pores, the holes on the fracture surface which were formed in the matrix with the removal of VGCF fragments from it, are clearly visible on the fracture surfaces of the composite films containing VGCF. These defects are practically absent on the fracture surfaces of the PI-I and PI-II compositions with CNC. But the fragments of the nanoparticles of this type, which were destroyed with the failure of materials, are visible in the fracture surfaces of these carbonized composites (Figure 5(b), (d)). These destructed CNC on the failure surface of the samples are additionally presented in the inserts.

During the determination of the mechanical characteristics of partially carbonized films, the clear dependence of the results on the storage conditions of the carbonized samples prior to their tests was noted. The characteristics, represented in Tables 3–5, are obtained on the films, tested immediately after the carbonization, or kept after carbonization in the exsiccator in the dry atmosphere. At the same time, the partially carbonized films, stored under the conditions of the natural humidity of air, became absolutely brittle and unfit for studies already after 2 days of storage. An assumption was advanced that the reason for this effect can be the excessive absorption of moisture from air by the carbonized film, which leads to the increase in its brittleness as a result of the realization of the Rehbinder effect (Piggotti, 1964).

For affirming this assumption, the change in the mass of films after their storage in air (Table 6) was measured: four samples of each type were tested. As can be seen from the results obtained, after the storage of partially carbonized film under the conditions of the natural humidity of air, substantially considerable increase in the mass of samples is observed than after the storage under the same

conditions of initial, not carbonized film. Let us note that during the storage of samples in dry air, their mass did not change. Obviously, the increase in the porosity of the composite film occurs at the early stages of its carbonization. This conclusion is confirmed by the SEM data: the microphotos (Figure 6) demonstrate the developed porosity, which is present on the surface of the carbonized composite films.

4. Conclusions

The kinetics of the carbonization of both the PI and composite films studied are strongly dependent upon the temperature–time regime of this process. The carbonization process under the conditions, used in this work, leads to the noticeable mass losses of the films studied—as high as 21–24%. These are the substantial mass loss values, if we will take into account that the full coke residues of the aromatic PI films of different structures after the carbonization–graphitization process in the inert atmosphere are as high as 40–50% (Bessonov et al., 1987). The mass losses of the composite films, based on both types of PI used, carbonized up to 500°C, are 1–3% less (depending on the nanofiller concentration) as compared to those of the unfilled films. But this apparent effect should be ascribed to the presence of some amount of the thermally stable carbon nanofiller in the composite material.

Comparing the structural characteristics of two PIs, used in the work, we can conclude that the PI-I films, which are characterized by the partially ordered structure, can be assumed to be a more promising precursor for conducting the carbonization process than the PI-II films with the weakly ordered structure. The carbonization of the PI-I films at 500°C makes it possible to obtain the films, characterized by deformation at break of ~0.5%, while the carbonization of the PI-II films under the same conditions leads to the formation of absolutely brittle products.

The uniform distribution of nanofiller's particles in the polymer volume was ensured while introducing both types of carbonic nanoparticles—CNC or VGCF in the concentrations up to 6 vol. % into the two PIs used. However, this modification leads to different changes in the hardness of two compared materials. Only a little increase in the modulus of the rigid-chain PI-I films is caused by the introduction of nanoparticles of both types into the polymer. The introduction of the same particles into the PI-II films leads to a more noticeable increase in the modulus.

Table 5. Mechanical properties of PI-based composite films carbonized up to different temperatures

N	PI and nanoparticles type, nanoparticles concentration (vol. %)	Films properties		
		E (GPa)	σ_b (MPa)	ε_b (%)
II-II	PI-II + 6 vol. % VGCF	3.62	134	12
II-II-500	PI-II + 6 vol. % VGCF + carbonization up to 500°C–60 min	5.09	54	1.2
II-II-550	PI-II + 6 vol. % VGCF + carbonization up to 550°C–60 min	6.69	30	0.8
II-III	PI-II + 15 vol. % VGCF	4.29	111	7
II-III-500	PI-II + 15 vol. % VGCF + carbonization up to 500°C–60 min	5.26	57	1.7
II-III-550	PI-II + 15 vol. % VGCF + carbonization up to 550°C–60 min	7.91	48	0.7

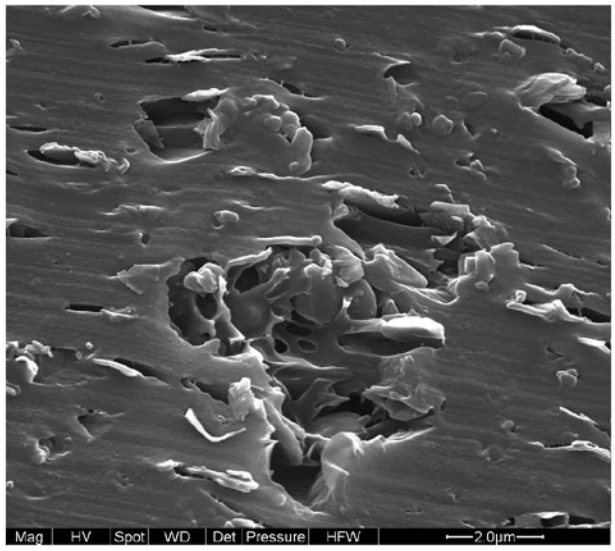

Figure 6. SEM image (×5000) of a fragment on the surface of the composite film PI-II + 6 vol. % CNC.

Table 6. Mass gain of pristine and partially carbonized PI and PI-based composite films caused by their storage in dry and normal room conditions

Film type	Storage period (days)	Atmosphere	Mass gain (%)
PI-II, pre-dried	20	Room air	+1.4
PI-II + 6 vol. % CNC, pre-dried	20	Room air	+2.1
PI-II + 6 vol. % CNC, carbonized 500°C–60 min	20	Dry air	0
PI-II + 6 vol. % CNC, carbonized 500°C–60 min	20	Room air	+4.0

The positive result of the introduction of CNC or VGCF into both PI films was the increase in the deformability of the obtained composite films in the partially carbonized state in comparison with the products of carbonization of the unfilled PI films. This effect appeared more and more significant along with the increase in the concentration of the nanoparticles in the polymer. The carbonization of the composite films based on the rigid-chain PI-I does not lead to any increase in the Young's modulus of the material, whereas the substantial increase in the modulus of the PI-II-based composite films was registered as a result of their carbonization in the same conditions.

The mechanical characteristics of the carbonized materials are strongly influenced by the conditions of their storage after carbonization. The presence of moisture in the atmosphere, in which these materials are stored, leads to the reduction of the deformation at break up to the complete embrittlement of the films.

Funding
This work was financially supported by Russian Foundation for Basic Research [project number 13-03-00547]; Russian Ministry of Education and Science within State Contract number 14.Z50.31.0002.

Author details
I.V. Gofman[1]
E-mail: gofman@imc.macro.ru
K. Balik[2]
E-mail: balik@irsm.cas.cz
M. Cerny[2]
E-mail: cerny@irsm.cas.cz
M. Zaloudkova[2]
E-mail: zaloudkova@irsm.cas.cz
M.Ja. Goikhman[1]
E-mail: goikhman@hq.macro.ru
V.E. Yudin[1]
E-mail: yudin@hq.macro.ru
[1] Institute of Macromolecular Compounds, Russian Academy of Sciences, Bolshoy pr. 31, St. Petersburg 199004, Russia.
[2] Institute of Rock Structure and Mechanics, Academy of Sciences of Czech Republic, V Holesovickach 41, 182 09 Prague 8, Czech Republic.

Citation information
Cite this article as: Peculiarities of the initial stages of carbonization processes in polyimide-based

nanocomposite films containing carbon nanoparticles, I.V. Gofman, K. Balik, M. Cerny, M. Zaloudkova, M.Ja. Goikhman & V.E. Yudin, *Cogent Chemistry* (2015), 1: 1076712.

References

Askadskii, A. A. (2003). *Lectures of physico-chemistry of polymers*. Hauppauge, NY: Nova Science.

Askadskii, A. A. (2005). *Computational materials science of polymers*. Cambridge: Cambridge International Science.

Bessonov, M. I., Koton, M. M., Kudryavtsev, V. V., & Laius, L. A. (1987). *Polyimides—Thermally stable polymers*. New York, NY: Plenum.

Dobrovol'skaya, I. P., Mokeev, M. K., Sazanov, Y. N., Gribanov, A. V., & Sukhanova, T. E. (2006). Changes in the supramolecular structure of heat-resistant polyimide fibers in the course of thermal treatment. *Russian Journal of Applied Chemistry, 79*, 1178–1180. http://dx.doi.org/10.1134/S1070427206070263

Doyama, M., Ichida, A., Inoue, Y., Kogure, Y., Nozaki, T., & Yamada, S. (2011). Partial carbonization of aromatic polyimide films. *International Journal of Inorganic Materials, 3*, 1105–1107.

Doyama, M., Takahashi, Y., Abe, H., Inoue, Y., Kogure, Y., Nozaki, T., & Yamada, S. (2003). Partial carbonization of aromatic polyimide films-aiming at solar cells. *Materials Science and Engineering: B, 99*, 131–133. http://dx.doi.org/10.1016/S0921-5107(02)00528-7

Gofman, I. V., Svetlichnyi, V. M., Yudin, V. E., Dobrodumov, A. V., Didenko, A. L., Abalov, I. V., ... Gusarov, V. V. (2007). Modification of films of heat-resistant polyimides by adding hydrosilicate and carbon nanoparticles of various geometries. *Russian Journal of General Chemistry, 77*, 1158–1163. http://dx.doi.org/10.1134/S1070363207070043

Gribanov, A. V., Sazanov, Y. N., & Mokeev, M. V. (2002). Role of structural characteristics of aromatic polyimides in carbonization. *Russian Journal of Applied Chemistry, 75*, 606–610. http://dx.doi.org/10.1023/A:1019573215648

Inagaki, M., & Feiyu, K. (2006). *Carbon materials. Science and engineering. From fundamentals to applications* (610 p.). Beijing: Tsinghua University Press.

Luo, Y., & Matsuo, M. (2010). Morphology of carbon/TiC composite films prepared by carbonization of polyimide/titania composites. *Polymer Bulletin, 64*, 939–951. http://dx.doi.org/10.1007/s00289-009-0230-0

Peponi, L., Puglia, D., Torre, L., Valentini, L., & Kenny, J. M. (2014). Processing of nanostructured polymers and advanced polymeric based nanocomposites. *Materials Science and Engineering: R: Reports, 85*, 1–46. http://dx.doi.org/10.1016/j.mser.2014.08.002

Perng, L.-H. (2000). Thermal decomposition characteristics of poly(ether imide) by TG/MS. *Journal of Polymer Research, 7*, 185–193. http://dx.doi.org/10.1007/s10965-006-0119-7

Piggotti, M. R. (1964). The rebinder effect. *Acta Metallurgica, 12*, 803–805. http://dx.doi.org/10.1016/0001-6160(64)90173-7

Smirnova, V. E., Gofman, I. V., Maritcheva, T. A., Yudin, V. E., Eto, K., Takeichi, T., ... Hishiyama, Y. (2007). The effect of different orientations in rigid rod polyimide films on the graphitized products. *Carbon, 45*, 839–846. http://dx.doi.org/10.1016/j.carbon.2006.11.012

Takeichi, T., Eguchi, Y., Kaburagi, Y., Hishiyama, Y., & Inagaki, M. (1999). Carbonization and graphitization of BPDA/PDA polyimide films: Effect of structure of polyimide precursor. *Carbon, 37*, 569–575. http://dx.doi.org/10.1016/S0008-6223(98)00223-1

Takeichi, T., Endo, Y., Kaburagi, Y., Hishiyama, Y., & Inagaki, M. (1998). Carbonization and graphitization of polyimide films: Effect of size of leaving group at imidization. *Journal of Applied Polymer Science, 68*, 1613–1620. http://dx.doi.org/10.1002/(ISSN)1097-4628

Valenkov, A. M., Gofman, I. V., Nosov, K. S., Shapovalov, V. M., & Yudin, V. E. (2011). Polymeric composite systems modified with allotropic forms of carbon (review). *Russian Journal of Applied Chemistry, 84*, 735–750. http://dx.doi.org/10.1134/S1070427211050016

Xie, X.-L., Mai, Y.-W., & Zhou, X.-P. (2005). Dispersion and alignment of carbon nanotubes in polymer matrix: A review. *Materials Science and Engineering: R: Reports, 49*, 89–112. http://dx.doi.org/10.1016/j.mser.2005.04.002

Zhang, B., Bershtein, V., Sukhanova, T., Zang, W., Chen, C., Egorova, L., ... Li, Y. (2012). Aromatic polyimide/MWCNT hybrid nanocomposites: Structure, dynamics, and properties. *Journal of Macromolecular Science, Part B, 51*, 1794–1814. http://dx.doi.org/10.1080/00222348.2012.659640